FINITE ELEMENT ANALYSIS IN FLUIDS

Proceedings of the Seventh International Conference on Finite Element Methods in Flow Problems

APRIL 3 – 7, 1989

The University of Alabama in Huntsville
Huntsville, Alabama

T. J. Chung, and Gerald R. Karr, Editors

UAH PRESS
DEPARTMENT OF MECHANICAL ENGINEERING
THE UNIVERSITY OF ALABAMA IN HUNTSVILLE
HUNTSVILLE, AL 35899

A FINITE-VOLUME COMPUTER PROGRAM FOR TURBULENT FLOW IN COMPLEX GEOMETRIES

Lars Davidson, Peter Hedberg, Erik Olsson
Applied Thermodynamics and Fluid Mechanics
Chalmers University of Technology
S-412 96 Gothenburg, SWEDEN

ABSTRACT

A computer code for complex geometries, written for general nonorthogonal coordinates, has been developed including a k-ϵ turbulence model. The basis of the program is briefly described below.

The Navier-Stokes equation can be written for general nonorthogonal curvilinear coordinates where the curvature effect of the mesh is inherent. The covariant velocity components are solved in our FVM formulation, which leads to the pressure-velocity coupling becoming relatively easy to handle at the expense of a more complicated expression of the convective and diffusive fluxes. When the velocity component, v_{1e} (or v_{2n}, see Fig. 1), is solved, the neighbouring velocities are projected in the direction of the velocity component v_{1e} (or v_{2n}). Thus we change the base vectors at the neighbouring points. This renders a simpler expression for the covariant derivatives. It should be stressed that when the procedure of changing the base vectors is carried out, it only affects the convected velocity. The convecting term (dot product of velocity and area) is calculated without any change of the base vectors. The same is true for the operator on the covariant velocity in the diffusion term.

For stability a hybrid central/upwind difference scheme is used. The discretised equations are written in a form enabling the TDM-Algorithm. The equations are solved using the SIMPLEC procedure.

It was shown in [1] that, when using upwind differencing, the use of projected velocities gives better results than when curvature effects are included in the source term.

The code is applied to two turbulent flows: the flow in a cascade, and the flow in a cavity with an inclined floor. The calculated results are compared with experimental data.

1. INTRODUCTION

This code has been developed by the two first authors, whose main research fields are turbulent flow in ventilated rooms and in turbomachines, respectively. The mathematical derivation of the formulation of the code is presented elsewhere [1], and the code is described in detail in [2]. The k-ϵ turbulence model has recently been implemented, and the code is currently being extended to be able to handle three-dimensional configurations.

2. FORMULATION

2.1 Momentum Equations

The momentum equations for turbulent flow in general co-ordinates, using covariant components can be written [1]

$$\frac{\partial v_i}{\partial \tau} + (\rho g^{jk} v_i v_j)_{,k} = -\frac{\partial p}{\partial x^i} + (\mu_{eff}\, g^{jk} v_{i,j})_{,k} \tag{1}$$

where g^{jk} denotes the contravariant components of the metric tensor. Here the subscripts (i,j,k) denote covariant components and superscripts (i,j,k) denote contravariant components and this convention is used throughout the paper. The comma notation is used for denoting covariant derivative. In [1] it was shown that if a local co-ordinate system is used so that the direction of the neighbouring velocities v_{inb} (i-co-ordinate direction, nb-neighbour)

A FINITE-VOLUME COMPUTER PROGRAM FOR TURBULENT FLOW IN COMPLEX GEOMETRIES

by

Lars Davidson, Peter Hedberg and Erik Olsson

Proc. 7th International Conference on Finite Element Methods in Fluid Problems, Huntsville, Alabama, pp. 390-395, 1989.

are kept the same as that of the velocity (v_{1e} or v_{2n}) being solved (see Fig. 1), Eq. (1) can be integrated and rewritten so that

$$\int_V \frac{\partial v_i}{\partial \tau} dV + \int_A g^{jk}(\rho v_i v_j - \mu_{eff} \frac{\partial v_i}{\partial x^j}) n_k dA + \int_A p\, n_i dA = 0 \qquad (2)$$

where A denotes the bounding area of the control volume with the volume V, and $\vec{n}$ is its normal vector.

It is well known that upwind differencing gives rise to numerical diffusion. For curved grids this becomes especially serious when the flow is across the grid. Even if the magnitude of the velocity component is well approximated by estimating the face value of v_1 (for example) with its node value, the direction of v_1 is not. This was recognised by Galphin et al. [3].

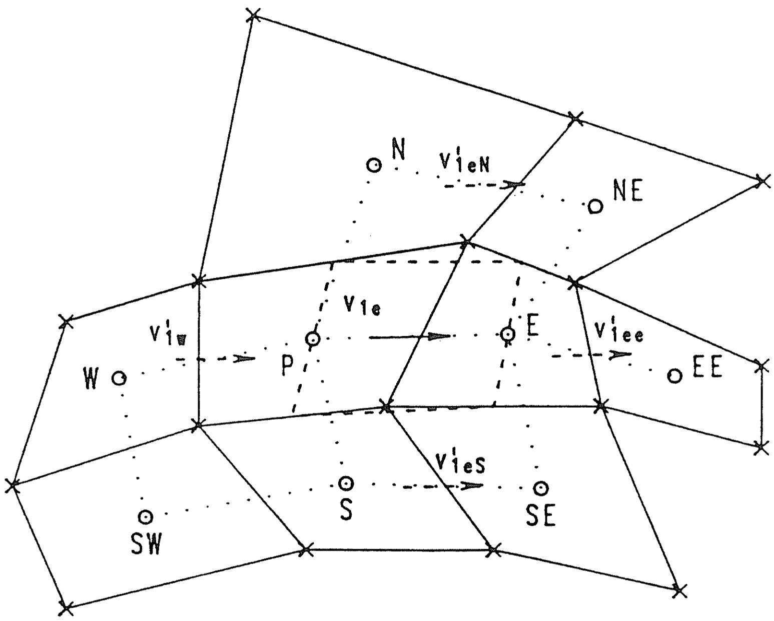

Figure 1. The grid (see Section 2.3). The dashed arrows show the neighbour velocity vectors projected on $\vec{PE}$, i.e. v'_{1ee}, v'_{1w}, v'_{1eN} and v'_{1eS}.

In the present formulation the velocity components in the immediate neighbourhood of the velocity component being solved, all have the same direction. This means that all the neighbours, v'_{1nb} (prime denotes velocity parallel to v_{1e}), of v_{1e}, have the same direction. In this way the problem of estimating a face value of v_1 having the in-correct direction is solved. The same is true for the v_2-equation. The procedure of projecting velocities drastically reduces the numerical errors due to upwind differencing associated with curved grids [1].

In most studies on deriving discretised equations for flow in complex geometries, the terms due to curvature, divergence and non-orthogonality of the grid have been included using Christoffel symbols and metric tensors. Since the number of these terms is rather large, it is very cumbersome and may also be inaccurate (there appears terms containing up to the third derivative of the grid coordinates). This is not the case with the present formulation.

2.2 k-ε Turbulence Model

The standard k-ε turbulence model is implemented in the code [2]. The equations for k and ε can be written

$$\int_V \frac{\partial \phi}{\partial \tau} dV + \int_A g^{jk}(\rho v_j \phi - \Gamma_{eff} \frac{\partial \phi}{\partial x^j}) n_k dA + \int_V b_\phi dV = 0 \qquad (3)$$

where $\phi = k$ or ϵ, and b_ϕ denotes the general source term, which for the k and ϵ-equations take the following forms:

$$b_k = \int_V (P_k - \rho\epsilon)\, dV;\quad b_\epsilon = \int_V \frac{\epsilon}{k} (C_{1\epsilon} P_k - C_{2\epsilon} \rho\epsilon)\, dV$$

where the production term, P_k, is calculated (without projecting the velocities) as

$$P_k = \mu_t (v_{i,j} + v_{j,i})\, g^{jk} v^i_{\ ,k}$$

The covariant derivatives of v_i and v^i are defined by [4]

$$v_{i,j} = \frac{\partial v_i}{\partial x^j} - \left\{ {k \atop i\ j} \right\} v_k$$

$$v^i_{\ ,j} = \frac{\partial v^i}{\partial x^j} - \left\{ {i \atop k\ j} \right\} v^k$$

The Christoffel symbol can be written [4]

$$\left\{ {\ell \atop i\ j} \right\} = \frac{1}{2} g^{k\ell} \left(\frac{\partial g_{ik}}{\partial x^j} + \frac{\partial g_{jk}}{\partial x^i} - \frac{\partial g_{ij}}{\partial x^k} \right)$$

The covariant components of the metric tensor g_{ij} are defined by [4]

$$g_{11} = g_{22} = 1;\quad g_{12} = \cos\alpha$$

where α is the angle between the base vectors $\vec{g}_1$ and $\vec{g}_2$.
The turbulent viscosity is calculated as

$$\mu_t = \rho C_\mu k^2/\epsilon$$

The constants in the turbulence model have been assigned their standard values [5]: $C_\mu = 0.09$, $C_{1\epsilon} = 1.44$, $C_{2\epsilon} = 1.92$, $\sigma_k = 1.0$, $\sigma_\epsilon = 1.3$

2.3 The Grid

A grid is shown in Fig. 1. The crosses define the corners of the scalar control volumes, and the circles define the scalar nodes. The position of a scalar node is defined as the average of its four cell corners. The lines which connect these nodes (dotted lines in Fig. 1) define the direction of the base vectors, $\vec{g}_i$.

The v_1-control volume is staggered in the positive x^1-direction; it is outlined with dashed lines in Fig. 1. Its east face, for example, is defined as being midway between the east faces of scalar control volumes P and E.

2.4 Discretization

Equation (2) can now be discretized using the control volume formulation described in [6]. For the v_1-equation the discretized equation may be written

$$a_P v_{1e} = \sum a_{nb} v'_{1nb} + b \qquad (4)$$

where the prime denotes velocity parallel to the v_{1e}-velocity. The v_2-equation is discretised in the same way. The a_E-coefficient in Eq. (4), for instance, contains convective contribution such as $(\rho\vec{v}\cdot\vec{A})_e$ and diffusive contribution such as $(\mu_{eff}\vec{A}\cdot\nabla)_e$ [cf. Eq. (2)], where $\vec{A}_e$ is the east face vector area of the control volume. The part of the diffusion terms which contains the cross-derivative due to non-orthogonality has been included in the source term, b.

To make it possible to solve the velocities using the usual TDM-Algorithm, Eq. (4) is rewritten so that

$$a_P v_{1e} = \sum a_{nb} v_{1nb} + b + b_{curv}$$

where the source term b_{curv} now contains

$$b_{curv} = \sum a_{nb} [v'_{1nb} - v_{1nb}]$$

The k and ϵ-equations [Eq. (3)] are discretized in the same manner, except that no curvature terms appear.

The equations are solved using the SIMPLEC-algorithm [7]. The four main features are staggered grids for the velocities; formulation of the difference equations in implicit, conservative form, using hybrid upwind/central differencing; rewriting of the continuity equation into an equation for the pressure correction; and iterative solving of the equations using TDMA.

2.5 Boundary Conditions

The velocities at the inlet were prescribed according to experiments; the turbulent quantities were estimated. Conventional wall-functions [5] were used for velocities, k and ϵ at all walls. Zero stream wise gradient was imposed for all variables at the outlet. At the symmetry plane the normal velocity component was set to zero, and the gradient in the normal direction of the remaining variables was set to zero.

3. RESULTS

3.1 Room With an Inclined Floor

The configuration with the grid is shown in Fig. 2. The calculated results are compared with experimental data from Hanel and Köthnig [8].

When the flow in ventilated rooms with small inlets is numerically simulated, it is not uncommon to prescribe the v_1-velocity at a line where x=constant [9,10], which means that fewer grid lines are needed in the inlet region. In the present calculation the v_1-velocity was prescribed at x/H=0.1, using the formula for the velocity in a wall jet [11]

$$v_1/U_{in} = [\cosh(\frac{y}{\delta_{1/2}} - 0.14)]^2 \qquad (5)$$

where $\delta_{1/2}$ is the half-width of the wall jet, and which was determined from the experiments [8]; Eq. (5) was used for grid lines which were nearer the ceiling than $\delta_{1/2}$.

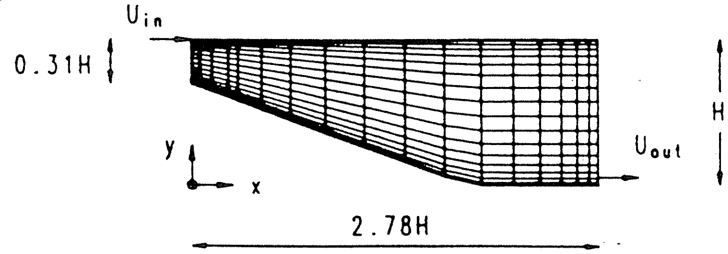

Figure 2. Configuration for the room with the grid (schematically drawn) included. The height of the inlet: h=0.009H; Reynolds number, $U_{in}h/\nu$= 3700.

In Fig. 3 the calculated velocity profiles are compared with the experimental data, and the agreement is good.

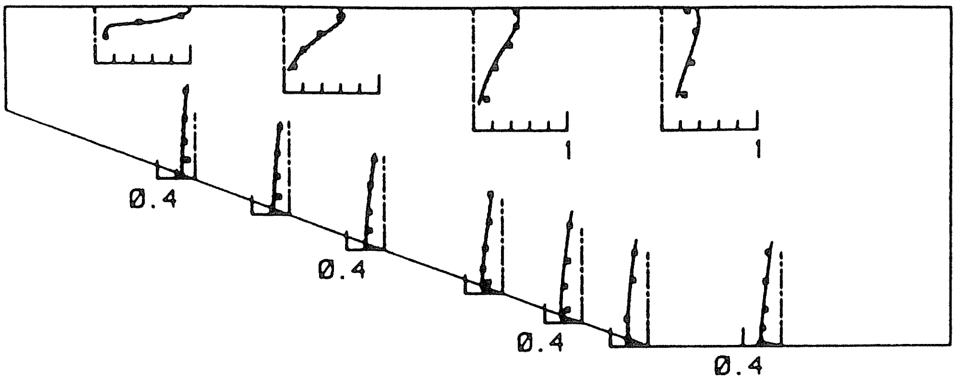

Figure 3. Velocity profiles of the absolute velocity, $|\vec{v}|/U_{in}$. Solid lines: 33x33 node grid; dotted lines: 53x62 node grid; markers: experiments [8].

3.2 Flow in a cascade

The cascade consists of two symmetric profiles located beside each other, aligned with the main flow direction in a closed wind tunnel. The experimental and numerical studies are a part of a turbomachinery project.

Because the experimental part of the project has started recently there is not much experimental data available. The Reynolds number based on the corda length is Re=1.6 10^6. The first half metre of the blade profile is an ellips where the main axes are 100 mm and 500 mm. The rear end of the profile is described by a 1500 mm long radius. The curvature is continuous. The centre lines of the blades are located 425 mm from each other. The height of the wind tunnel test section is 1250 mm. Figure 4 shows the mesh in the calculation and Fig. 5 shows calculated data and experimental data [12] for C_p. The calculation predicts a separation at about 15 cm from the trailing edge. This explains the differences in C_p at the end of the profile. The underlying reason is probably that the wall function over-estimates the value of the wall shear stress with the present pressure gradient. Obviously some other way of estimating the shear stress has to be thought of as the project proceeds.

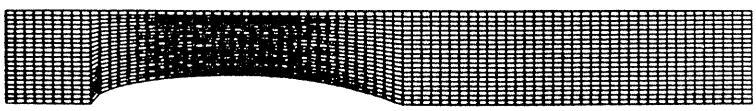

Figure 4. Grid for the cascade.

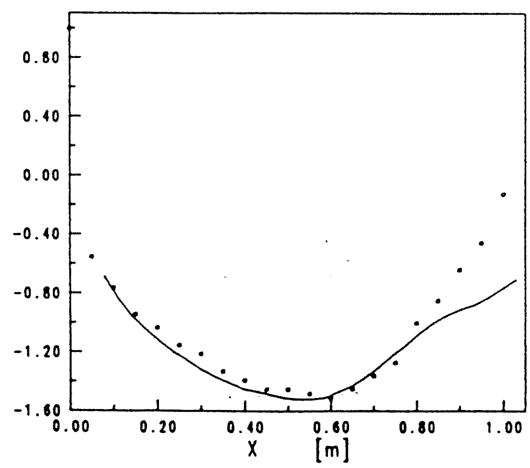

Figure 5. Pressure coefficient, C_p, as function of corda length, X.

ACKNOWLEDGEMENTS

This work was financed by the Swedish Council for Building Research, the Swedish Board for Technical Development, and by many Swedish companies with interest in turbomachinery technology.

REFERENCES

1. DAVIDSON, L. and HEDBERG, P., "Mathematical Derivation of a Finite-Volume Formulation for Laminar Flow in Complex Geometries", accepted for publication in International Journal for Numerical Methods in Fluids, August, 1988.

2. DAVIDSON, L. and HEDBERG, P., "FLUX2D: A Finite-Volume Computer Program Written in General Non-Orthogonal Coordinates for Calculation of Two-Dimensional Turbulent Flow", Rept. 88/1, Dept. of Applied Thermodynamics and Fluid Mechanics, Chalmers University of Technology, Göteborg, 1988.

3. GALPHIN, P.F., RAITHBY, G.D. and VAN DOORMAAL, J.P., "Discussion of Upstream-Weighted Advection Approximations for Curved Grids", Numer. Heat Transfer, Vol. 9, pp. 241-246 (1986).

4. FLUGGE, W., "Tensor Analysis and Continuum Mechanics", Springer-Verlag, Berlin, 1972.

5. RODI, W. "Turbulence Models and their Application in Hydraulics", International Association of Hydraulic Research, Monograph, Delft, 1980.

6. PATANKAR, S.V., "Numerical Heat Transfer and Fluid Flow", McGraw-Hill, Washington, 1980.

7. VAN DOORMAAL, J.P. and RAITHBY, G.D., "Enhancements of SIMPLE Method for Predicting Incompressible Fluid Flows", Numer. Heat Transfer, Vol. 7, pp. 147-163, 1984.

8. HANEL, B., KÖTHNIG, "Methoden zur Vorausbestimmung von Strömungsvorgängen in klimatisierten Räumen", Luft- und Kältetechnik, Vol. 3, pp. 136-140, 1983.

9. DAVIDSON, L. and OLSSON, E., "Calculation of Age and Local Purging Flow Rate in Rooms", Bldg. Environ., Vol. 22, p. 111, 1987.

10. DAVIDSON, L. and OLSSON, E., "Calculation of some Parabolic and Elliptic Flows Using a New One-Equation Turbulence Model", p. 411, Vol. 1, Part 1, 5th Int. Conf. on Numerical Methods in Laminar and Turbulent Flow, Eds. C. Taylor, W. G. Habashi and M. M. Hafez, Montreal, 1987.

11. SCHWARTZ, W.H. and COSART, W.P., "The Two-Dimensional Turbulent Wall-Jet", J.F.M., Vol. 10, Part 4, p. 481, 1961.

12. JOHANSSON, K.B., private communication, Dept. of Applied Thermodynamics and Fluid Mechanics, Chalmers University of Technology, Göteborg, 1988.